Simulation of modern and glacial climates with a coupled global model of intermediate complexity

Andrey Ganopolski, Stefan Rahmstorf, Vladimir Petoukhov & Martin Claussen

Potsdam Institute for Climate Impact Research (PIK), PO Box 60 12 03, 14412 Potsdam, Germany

A global coupled ocean–atmosphere model of intermediate complexity is used to simulate the equilibrium climate of both today and the Last Glacial Maximum, around 21,000 years ago. The model successfully predicts the atmospheric and oceanic circulations, temperature distribution, hydrological cycle and sea-ice cover of both periods without using 'flux adjustments'. Changes in oceanic circulation, particularly in the Atlantic Ocean, play an important role in glacial cooling.

Simulation of the icy climate of the Last Glacial Maximum (LGM) is one of the main challenges facing climate modellers. Until now, ocean models and atmosphere models have been used separately to reproduce aspects of glacial climate. For the atmospheric model simulations the sea surface temperature (SST) needs to be specified in some way, and two approaches have been used for this. The first is to use data-based reconstructions of glacial sea surface temperatures (for example, the CLIMAP reconstruction[1]) as a boundary condition; eight simulations of this type are at present being evaluated in the palaeoclimate model intercomparison project (PMIP)[2]. These experiments are diagnostic in the sense that the surface temperature of two-thirds of the planet is prescribed and no closed heat budget exists (a net global heat flux from ocean to atmosphere typically arises, shown, for example, as 4×10^{14} W in ref. 3).

The second approach is to compute SST by assuming a slab ocean of 50 m thickness with fixed (present-day or similar) heat transport; six of the PMIP simulations fall in this category, as well as the one recently published by Webb *et al.*[3]. However, there is no basis for assuming near-modern ocean heat transport values in a radically different climate, except as a sensitivity experiment. Ocean model studies[4–6] and sediment core data[7–9], as well as our coupled simulation, suggest that ocean circulation during the LGM was different from today's, particularly the Atlantic 'conveyor belt', the main transporter of heat. Even if the circulation remained the same, changed temperatures would alter the heat transport.

Ocean-only model simulations suffer a similar limitation to the atmosphere-only models: they have to specify glacial surface conditions. For a credible simulation of the glacial (or any other) climate state, which predicts rather than assumes the surface temperature distribution, only coupled ocean–atmosphere models can be used. Coupled general circulation models (GCMs) are routinely used to simulate present climate and to study climate variability and possible anthropogenic changes. But most of these models still use *ad hoc* flux adjustments at the air–sea interface, which makes questionable the application of these models to climate states far from the present. Furthermore, the long (diffusive) adjustment timescale of the deep ocean requires an equilibration time of several thousand years. It is still impractical today to integrate a coupled circulation model for that long, because of the prohibitive computational cost arising from the short time-steps needed to resolve weather in the atmosphere.

We have sought a way out of this dilemma by developing an efficient climate model of intermediate complexity, which does not resolve individual synoptic weather systems but parametrizes their effects and contains the most important climate processes and feedbacks. With this model we have conducted equilibrium simulations of both modern and glacial climate; the latter was forced by a change in solar forcing, a reduced atmospheric CO_2 concentration and prescribed continental ice sheets corresponding to 21,000 yr before present. The main characteristics of the model's glacial climate, described in detail in the following sections, are a global cooling of 6.2 °C, a cooling of the tropics of 3.8 °C (4.6 °C over land), an increase in Northern Hemisphere westerlies and trade winds, a southward shift of North Atlantic Deep Water (NADW) formation, a penetration of Antarctic Bottom Water (AABW) into the northern North Atlantic, and a substantially reduced oceanic heat transport into the high latitudes of the North Atlantic with a corresponding southward movement of the sea-ice margin to between 50° and 60° N.

Model and coupling procedure

The CLIMBER-2 model used in this study[10] is a low-resolution coupled climate–biosphere model and was developed at the Potsdam Institute for Climate Impact Research (PIK) for long-term simulations. The biosphere module was not used in this study; instead, the fraction of vegetation was prescribed based on empirical data for modern conditions. Biospheric feedback will be considered in a future study.

The atmosphere module is a substantially improved version of the dynamical–statistical atmosphere model of Petoukhov and Ganopolski[11], with 10° latitudinal and 51° longitudinal resolution. Each grid cell can have arbitrary land and ocean fractions for which calculations are performed separately. The model explicitly resolves the large-scale circulation patterns: subtropical jet streams, Hadley, Ferrel and polar cells, monsoon and Walker circulations, tropospheric quasi-stationary planetary waves, and centres of action such as the Siberian high-pressure area and the Aleutian low-pressure area. It does not resolve individual synoptic weather systems but rather predicts their statistical characteristics, including the fluxes of heat, moisture and momentum associated with ensembles of synoptic systems. The vertical structure includes a planetary boundary layer, a free troposphere (including cumulus and stratiform clouds) and a stratosphere. Radiative fluxes are computed on 16 vertical levels. In short, the model works like most GCMs except that synoptic-scale activity is parametrized, which allows much longer time steps and coarse resolution.

The ocean module is a zonally averaged model with three separate basins (Atlantic, Indian and Pacific oceans) similar to the one used by Stocker *et al.*[12], with parametrizations of the vorticity balance and of Ekman transport. It includes a thermodynamic sea-ice model

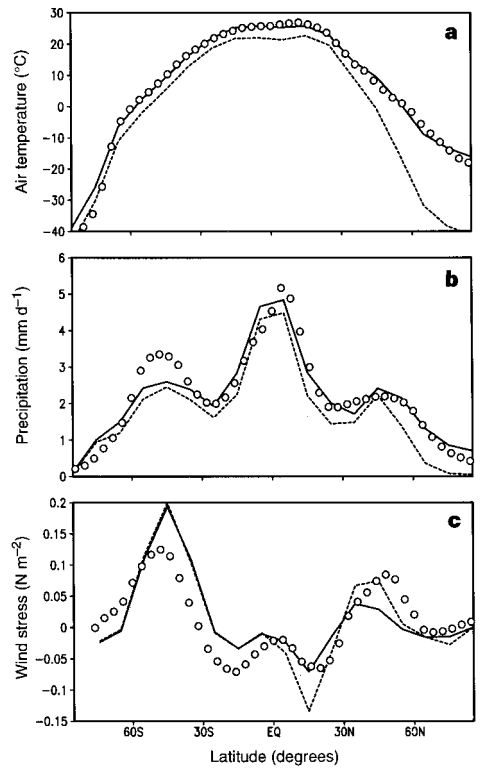

Figure 1 Zonally averaged annual-mean characteristics: **a**, air temperature; **b**, precipitation; **c**, wind stress over the oceans. The solid line shows results of the coupled model for the present climate, and the dashed line for the glacial climate. The dots indicate observed modern values[45,46]. Model output is averaged over the last 100 years of the 5,000-year simulation. We note the decrease in temperature and precipitation, and the increase in wind stress, in the glacial climate.

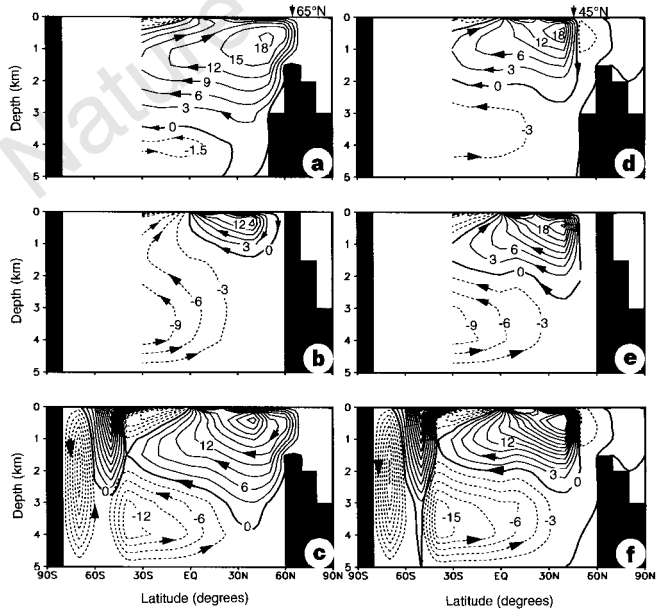

Figure 2 Meridional transport stream function for the Atlantic (top), Indo-Pacific (middle) and global ocean (bottom). The left-hand column (**a–c**) shows the modern circulation, and the right-hand column (**d–f**) shows the glacial circulation as simulated by the coupled model. Contour values are in Sv (1 sverdrup = $10^6\,m^3\,s^{-1}$).

which predicts the sea-ice fraction and thickness for each grid cell, with simple treatment of advection and diffusion of sea ice.

Ocean and atmosphere interact via surface fluxes of heat, fresh water and momentum. Freshwater fluxes into the ocean include continental runoff, routed by assigning an ocean grid cell to each land cell. Glaciers are assumed to be in equilibrium, and glacier runoff is computed as the difference between annual accumulation and ablation; it is added to the mass of sea ice in corresponding ocean areas.

The relative simplicity of the model allows coupled long-term simulations to be performed, for example the calculation of a climate equilibrium state that is not close to the initial conditions. The price to pay for the high computational speed is that only the large-scale, time-averaged properties of climate are captured. Unlike GCMs, our model cannot simulate weather, many natural variability modes (such as El Niño/Southern Oscillation), or regional details. The ocean module resolves only the vertical circulation (Ekman cells and thermohaline flow), whereas zonal gradients within each ocean are ignored and the heat and salt transports of the horizontal circulation are parametrized as simple diffusion terms.

Ocean and atmosphere modules were validated separately for the present climate against observed data, using traditional surface boundary conditions (prescribed SST and sea-ice fraction for the atmosphere module, relaxation towards observed SST and salinity for the ocean module). Both model components reproduce reasonably well the chief characteristics of the present climate state (for example, temperature, precipitation, cloudiness, energy fluxes, atmospheric and thermohaline ocean circulation), within the range shown by GCMs. In addition, systematic comparisons showed that the ocean component has a very similar response to changes in freshwater forcing as an ocean GCM[13]. An important diagnostic used in tuning the atmosphere module is the implied oceanic heat and freshwater transport (computed as an integral of air–sea fluxes), which needs to be well represented in order to allow successful coupling[14].

The models were then coupled without any flux adjustments and the equilibrium climate was computed by integrating the coupled system synchronously for 5,000 model years with a fixed atmospheric CO_2 concentration of 280 p.p.m. corresponding to modern (pre-industrial) conditions. In the glacial experiment, the annual cycle of insolation was changed, the atmospheric CO_2 concentration was reduced to 200 p.p.m., continental ice sheets[15] were prescribed (and consequently the sea level was lowered by 105 m and global salinity increased by 1.0 practical salinity units, p.s.u.) to reflect conditions 21,000 yr before the present (these are the standard LGM boundary conditions defined by the PMIP[2] project). Again, the coupled model was integrated for 5,000 model years to reach climate equilibrium.

Modern climate

After coupling, the model settled into a climate state close to that of the uncoupled component models. Some zonally averaged, annual-mean characteristics of the coupled climate are shown in Fig. 1. Seasonal variations of quantities such as temperature, precipitation, evaporation and ice cover are not shown here, but are also in good agreement with observations, as is the contrast between land and ocean areas.

The Atlantic Ocean (Fig. 2a) in the coupled simulation forms $20 \times 10^6\,m^3\,s^{-1}$ (20 sverdrups (Sv)) of NADW, 10 Sv of this NADW flow into the circumpolar ocean at 30° S between 1.5 and 3.5 km depth. Between 4 and 5 km depth, 2 Sv of AABW enter the Atlantic from the south. These numbers are within the range of present oceanographic estimates[16,17]. Flow in the Indian and Pacific oceans (Fig. 2b) is dominated by inflow from the south below 3 km depth, upwelling and southward return flow between 1.5 and 3 km depth (consistent with tracer data[18]), and northward inflow of inter-

mediate water across 30° S above 1.5 km depth. The global stream function (Fig. 2c) in addition shows the overturning cells of the Southern Ocean[19]: the Deacon cell (30 Sv) and the Antarctic cell (19 Sv).

The vertical salinity structure of the Atlantic (Fig. 3a) is crucial for the freshwater transport and stability of the 'conveyor belt'[20]; it shows the characteristic fresh tongue of Antarctic Intermediate Water at around 1 km depth, in agreement with observations[21]. Oceanic heat transports are shown in Fig. 4a–c. The Atlantic heat transport is northward throughout, peaking at 1.2 PW at 20° N in agreement with oceanographic measurements[22]. The combined Pacific and Indian Ocean heat transport is poleward in both hemispheres, as observed[23].

Climate equilibria for present-day forcing

For present-day forcing conditions, our coupled model has the same two climate equilibrium states which were previously found in the coupled GCM of Manabe and Stouffer[24], namely with NADW formation (Fig. 2a) and without (not shown). Which of these distinct states is reached depends on the initial conditions. The state without NADW formation shows a region of cooling (relative to the present climate) centred on the northern North Atlantic with a maximum of 8 °C (annual mean), with a very similar pattern but slightly weaker than that of ref. 24 (10 °C). This cooling is much stronger in winter (up to 20 °C in February).

These two different climate states provide an important sensitivity test for our atmosphere module when compared with GCM results. Our model obtains not only the same kind of temperature changes, but also very similar changes in precipitation, sea-level pressure and atmospheric circulations as the Manabe and Stouffer GCM. As an example we show the atmospheric meridional mass transport and its changes in Fig. 5. Further sensitivity studies (for example, global warming scenarios) have been performed which likewise show good agreement of our model with GCM simulations;

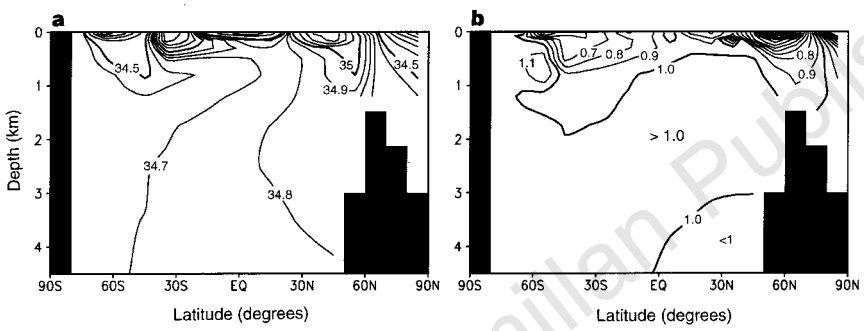

Figure 3 Zonal mean salinity in the Atlantic for the modern climate (**a**) and the difference between glacial and modern climates (**b**). The tongue of fresh Antarctic Intermediate Water spreading north at 1 km depth is shown in **a**. We note that global mean salinity in **b** was increased by 1.0 p.s.u. owing to fresh water being locked up in ice sheets; a salinity increase of <1 p.s.u. thus corresponds to a relative salinity decrease in its effects on circulation.

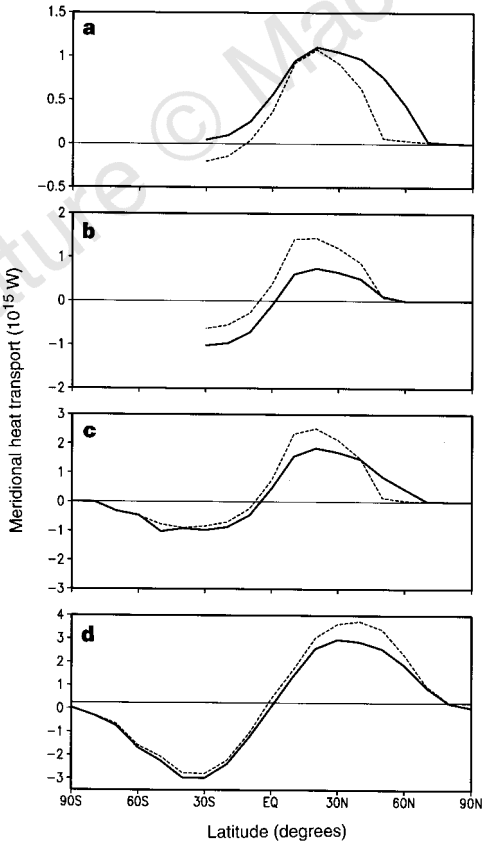

Figure 4 Meridional heat transport curves for the Atlantic (**a**), the Indo-Pacific (**b**), the global ocean (**c**) and the atmosphere (**d**). Solid lines show the simulated modern climate, dashed lines the glacial climate.

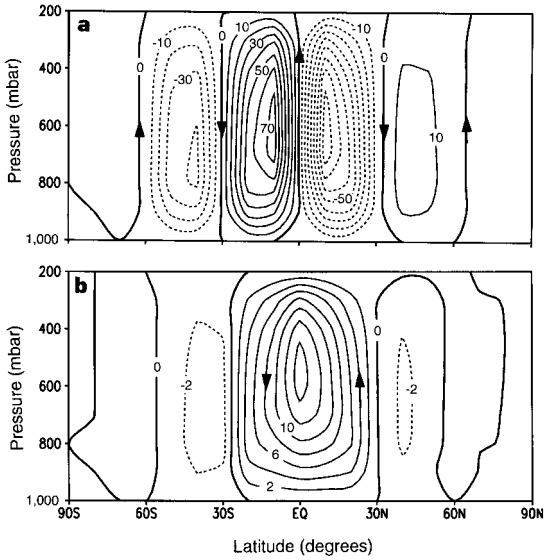

Figure 5 Annual-mean atmospheric meridional mass transport in units of 10^9 kg s^{-1}. **a**, The present climate; **b**, the difference of a climate with and without NADW formation. This difference represents a strengthening of the Northern Hemisphere Hadley circulation and a southward shift of the intertropical convergence zone (ITCZ) when NADW formation is turned off. Compare Fig. 26 of ref. 24.

these will be reported in detail elsewhere. The model's climate sensitivity to a doubling of atmospheric CO_2 content is 3.0 °C, in the middle of the range given by the IPCC[25].

Glacial climate

When the LGM boundary conditions are imposed, a glacial climate is simulated that is on average 6.2 °C colder (surface air temperature) than the modern (pre-industrial) climate. The spatial and seasonal distribution of the cooling is shown in Fig. 6. The strongest cooling (up to 30 °C) is over the North Atlantic and Europe in winter; in summer there are two slightly weaker maxima over the ice sheets of the northern continents. Zonal mean cooling (Fig. 7a) is up to 25 °C north of 60° N and declines towards the south, reaching just under 5 °C at the Equator and 3–5 °C in most of the Southern Hemisphere.

The tropical cooling in our coupled run is partly due to increased oceanic heat transport out of the tropics (Fig. 4a–c): the oceans transport an additional 0.7 PW northwards across 20° N in glacial conditions, whereas southward transport across 20° S is reduced slightly (Fig. 4c). The increased northward ocean heat transport out of the tropics is partly due to the enhanced meridional temperature gradient and partly due to enhanced Ekman circulation as a consequence of the stronger Northern Hemisphere trade winds. An experiment without these ocean heat transport changes (with slab ocean, discussed below) shows much less tropical cooling (Fig. 7). Further tropical cooling is due to atmospheric changes, mainly the reduction of atmospheric water vapour and CO_2 concentrations and increased atmospheric heat transport towards northern middle latitudes (0.3 PW across 20° N, Fig. 4d).

Our model predicts substantial changes in the hydrological cycle (Fig. 6c, d). As in all models, precipitation simulations are less reliable than temperature predictions and must be interpreted with caution. Nevertheless, several significant features stand out which are also reflected in proxy data: a drying of the tropics[26] and northern high latitudes[27], a strongly reduced Asian summer monsoon[28], and increased winter precipitation in some (sub)tropical regions[26]. Global mean precipitation is reduced by 16% from 2.65 to 2.23 mm d^{-1}.

The main changes in atmospheric circulation are a strengthening of the Northern Hemisphere westerlies[27] and trade winds[29] (Fig. 1c) and a southward shift in the storm track over the Atlantic (visible in the precipitation change pattern in Fig. 6c) in response to the sea-ice advance.

The simulated ocean circulation changes in the Atlantic (Fig. 2d)—southward shift of convection sites, shallower outflow of NADW, northward penetration of AABW—agree with recent reconstructions of glacial ocean circulation[9,30]. We note that the overall rate of NADW formation, and its outflow into the Southern Ocean, is only slightly reduced, consistent with radiochemical data[31]. The shallower NADW flow is caused by a relative salinity and density reduction in NADW compared with AABW (Fig. 3b); the flow rate does not change much because relative salinity in the South Atlantic decreases as much as in the north, and the flow depends on the north–south density gradient[20]. In the Pacific

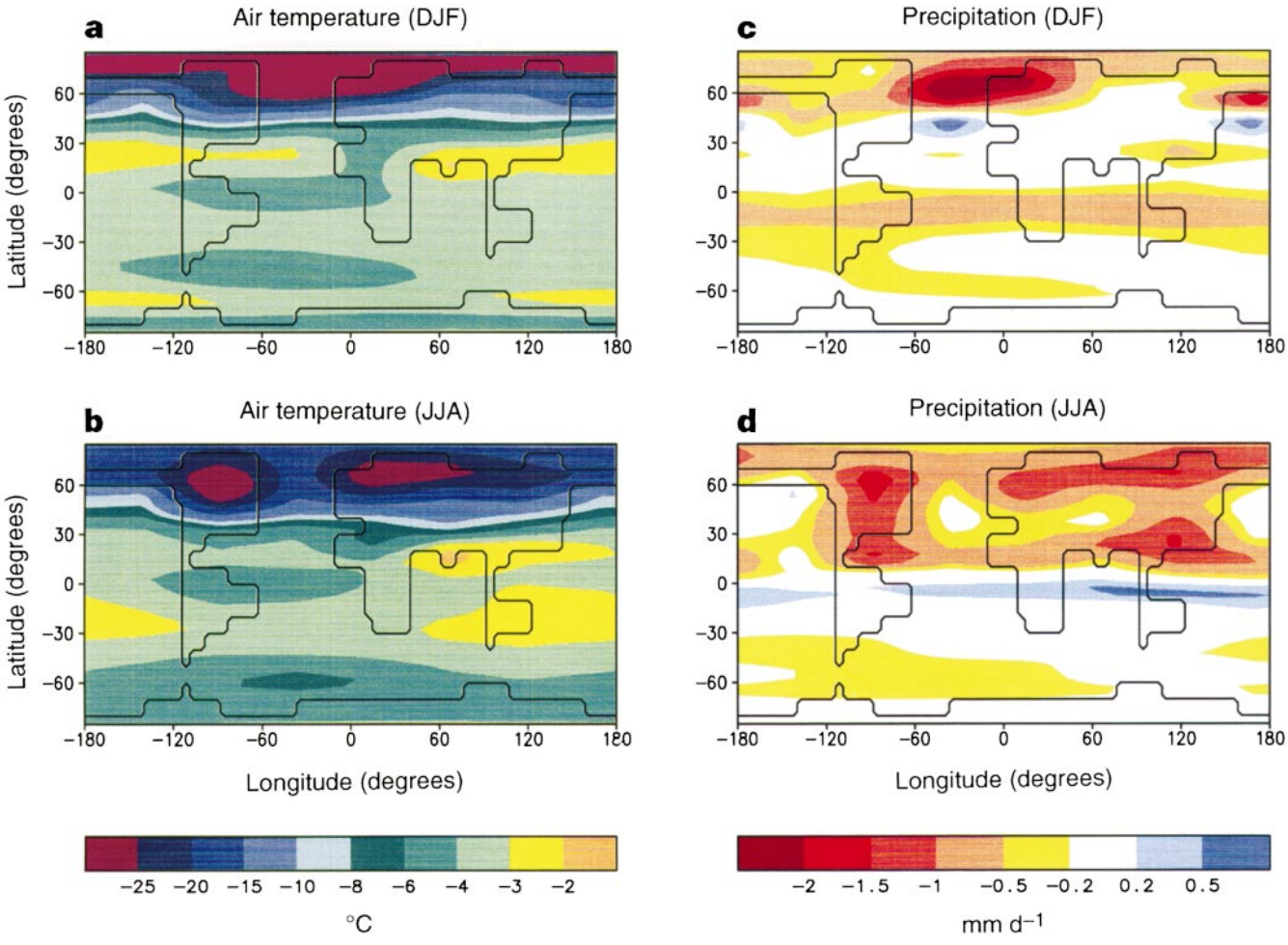

Figure 6 Temperature (**a**, **b**) and precipitation (**c**, **d**) changes in the glacial simulation relative to the modern climate simulation (LGM minus modern). Top panels show the northern winter months (December, January, February; DJF), bottom panels show the summer months (June, July, August; JJA).

(Fig. 2e) there is little change in abyssal circulation, but the formation of intermediate water in the North Pacific is increased to the extent that Atlantic and Pacific oceans have a similar thermohaline circulation in glacial conditions[32], quite unlike today. Formation of AABW (Fig. 2f) increases from 19 to 22 Sv.

For comparison, a simulation with a 50-m slab ocean and fixed (modern) ocean heat transport was performed. This represents a case where the ocean circulation plays no role in glacial cooling: slab ocean temperatures are determined strictly locally and do not depend on temperature changes elsewhere in the ocean; climate changes can be communicated only through the atmosphere. Whereas the present climate differs little between slab ocean and coupled simulation, global cooling for the LGM in the slab-ocean experiment was only 4.7 °C. This shows that changes in the ocean circulation enhance global cooling by 30% in our model (in the Northern Hemisphere the cooling is even enhanced by 50%). This may seem surprising at first, given that in equilibrium the ocean cannot be a global heat sink but merely transports heat from one place to another. However, the ocean circulation can influence the global heat budget, for example through the albedo of sea ice. In the modern climate, the northern Atlantic is kept ice-free up to high latitudes (~75° N in our model, in good agreement with satellite data) owing to the northward heat transport of the thermohaline circulation. In our glacial simulation, the sites of convection and formation of NADW shifted to south of 50° N (Fig. 2d) and so did the heat release by the ocean (Fig. 4a). The sea-ice margin moved southwards to between 50° and 60° N in winter, consistent with the CLIMAP[1] reconstruction. This increased the albedo and enhanced the high-latitude cooling by up to 10 °C relative to the slab-ocean case (zonal and annual mean, Fig. 7a).

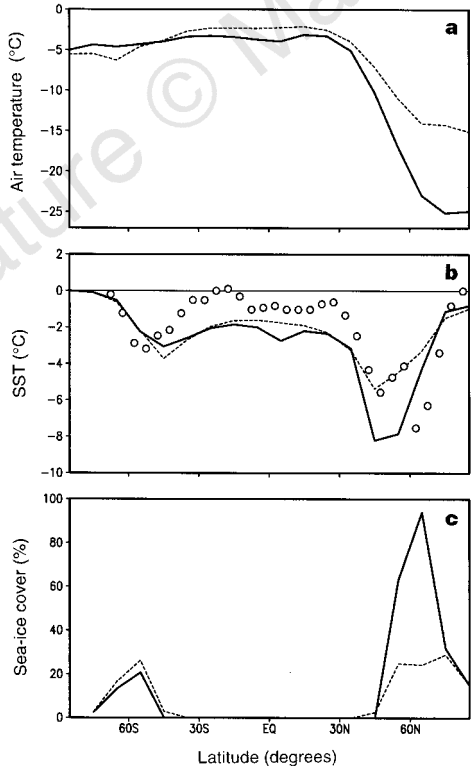

Figure 7 Glacial changes in three characteristics simulated with the coupled model (solid line) and the slab ocean (dashed line). **a**, Zonal mean surface air temperature; **b**, SST; **c**, percentage of sea-ice cover. The dots in **b** show the CLIMAP[1] reconstruction, which is much warmer in low latitudes than our model.

It is important to note that the cooling here does not result from an overall reduction in NADW formation, but merely from a southward shift of convection sites (as discussed by Rahmstorf[33] for a three-dimensional ocean model). The extent of sea ice and the sites of oceanic convection thus seem to be crucial regulators of climate in the northern middle and high latitudes, and even affect temperatures globally. The position of the ice margin is partly determined by oceanic heat transport; on the other hand the ice margin limits how far northward the ocean can transport heat. This interplay between ocean circulation and sea ice provides an important feedback which is linked to the ice–albedo feedback. It is only crudely modelled in our model, and regional details may become important. However, we speculate that the situation in many three-dimensional circulation models is also problematic: owing to difficulties with the representation of NADW overflow over the Greenland–Iceland–Scotland sill[34], these models tend to form NADW south of the sill far from the sea-ice margin, so that ice margin and thermohaline circulation become effectively decoupled. This may partly explain why even large reductions in NADW formation in global-warming scenarios (see, for example, refs 35 and 36) seem to have surprisingly little effect on climate[37].

Our slab-ocean experiment is comparable to the equivalent PMIP[2] simulations with atmospheric GCMs, and we obtain a cooling within the range simulated by the PMIP models. Much larger cooling (8.1 °C globally) was simulated only by the Goddard Institute for Space Studies (GISS) model[3], which seems to have a higher climate sensitivity than other models. The larger global cooling in the GISS model is due to a much colder Southern Hemisphere with massive sea-ice advance into middle latitudes. The largest zonal mean SST reduction in that model (8 °C) is found at 43° S. In our experiments, glacial cooling is much stronger in the Northern than in the Southern Hemisphere, and the meridional cooling pattern of the coupled model agrees well with the CLIMAP reconstruction except for the colder tropics (Fig. 7b).

Comparison with palaeoclimate data

Our simulation of the glacial climate is, to our knowledge, the first in which atmospheric and oceanic circulation are free to evolve together and find their own equilibrium climate. Changes in ocean circulation thereby lead to enhanced glacial cooling, notably in the North Atlantic region but also in the tropics. But how realistic are these results?

In the tropical belt, the CLIMAP reconstruction gives a sea surface cooling of only 1–2 °C, with some areas even warmer than at present. This is hard to reconcile with land data[38,39] showing cooling of ~5 °C. More recent marine data provide increasing evidence for a stronger cooling of the tropical oceans[40,41]. In our coupled model, the tropics cool by an average 4.6 °C over land, consistent with the data. The cooling in SST between 20° S and 20° N is 3.3 °C in the Atlantic, 2.4 °C in the Pacific and 1.3 °C in the Indian Ocean. These values fall between the cold coral data[40,41] and the relatively warm CLIMAP data. The fact that cooling is largest in the tropical Atlantic is in accord with palaeotemperature reconstructions[42].

In the North Atlantic region and over Europe the differences between the coupled simulation and the one with slab ocean are largest, as oceanic heat transport towards the northern North Atlantic is dramatically reduced in the coupled model. Again, the palaeoclimate data show no consensus in this region, with more recent data[43] indicating colder conditions than previously thought (see, for example, ref. 44). Peyron *et al.*[43] distinguish a northwestern zone, north of the Pyrenees–Alps line, with an annual cooling of 12 ± 3 °C and a maximum winter cooling of 30 ± 10 °C, and a Mediterranean zone with an annual cooling of 10 ± 5 °C, and

15 ± 5 °C cooling in the coldest month. It is difficult to compare these regional values with our low-resolution model as there is a strong gradient over Europe. Nevertheless, for northern Europe we get values close to those quoted above (Fig. 6), including the enhanced winter cooling and the pronounced drying found in the climate reconstruction from pollen data[43]. For the Mediterranean zone (~40° N) the annual cooling is 8 °C in our model and thus within the error margin of the data; in agreement with the pollen data, we get only a moderate drying in this region.

Overall, our coupled simulation supports a relatively cold glacial climate as is emerging from the most recent palaeoclimate reconstructions. Comparison with our slab-ocean experiment shows that this is due to changes in the ocean circulation in the Atlantic, and not to a high climate sensitivity of the atmosphere model (as reference point, the equilibrium sensitivity of our model to a doubling of atmospheric CO_2 is 3.0 °C globally and 2.4 °C for the tropics).

Implications

The successful simulation of both modern and glacial climates with the same coupled model, in which the component models have only been tuned separately and for modern conditions and where no flux adjustments were used, demonstrates the ability of climate models to predict radically different climate states. This is an important precondition for a greater credibility of global warming computations.

Although our results are highly encouraging, they can only be a first step. More simulations with increasingly detailed models, as well as improved palaeoclimate data, will be required to arrive at a robust quantitative understanding of glacial climate. We also point out that in our simulation the continental ice sheets and atmospheric CO_2 concentration were prescribed. A complete climate-system model should be able to predict the growth of ice sheets and the carbon cycle. Ultimately, the challenge is thus to produce a simulation of glacial cycles driven only by the Milankovic cycles in solar forcing. □

Received 4 June; accepted 1 December 1997.

1. CLIMAP Project Members. Seasonal reconstruction of the Earth's surface at the last glacial maximum. (Map Chart Ser. MC-36, Geol. Soc. Am., Boulder, 1981).
2. Joussaume, S. & Taylor, K. E. in *Proc. 1st Int. AMIP Scientific Conf., Monterey* 425–430 (World Climate Research Project, 1995).
3. Webb, R. S., Rind, D. H., Lehman, S. J., Healy, R. J. & Sigman, D. Influence of ocean heat transport on the climate of the last glacial maximum. *Nature* **385,** 695–699 (1997).
4. Fichefet, T., Hovine, S. & Duplessy, J. C. A model study of the Atlantic thermohaline circulation during the last glacial maximum. *Nature* **372,** 252–255 (1994).
5. Seidov, D., Sarnthein, M., Stattegger, K., Prien, R. & Weinelt, M. North Atlantic ocean circulation during the last glacial maximum and subsequent meltwater event—a numerical model. *J. Geophys. Res. C* **7,** 16305–16332 (1996).
6. Winguth, A. M. E., Maier-Reimer, E., Mikolajewicz, U. & Deplessy, J.-C. On the sensitivity of an ocean general circulation model to glacial boundary conditions. *Paleoceanography* (submitted).
7. Boyle, E. A. & Keigwin, L. D. Deep circulation of the North Atlantic over the last 200,000 years: Geochemical evidence. *Science* **218,** 784–787 (1982).
8. Curry, W. B., Duplessy, J. C., Labeyrie, L. D. & Shackleton, N. J. Changes in the distribution of $\delta^{13}C$ of deep water ΣCO_2 between the last glaciation and the Holocene. *Paleoceanography* **3,** 317–341 (1988).
9. Sarnthein, M. *et al.* Variations in Atlantic surface paleoceanography, 50–80N: A time slice record of the last 30,000 years. *Paleoceanography* **10,** 1063–1094 (1995).
10. Petoukhov, V. *et al.* CLIMBER-2: A climate system model of intermediate complexity. *Clim. Dyn.* (submitted).
11. Petoukhov, V. K. & Ganopolski, A. V. *A Set of Climate Models for Integrated Modelling of Climate Change Impacts* 1–96 (IIASA, Laxenburg, 1994).
12. Stocker, T. F., Wright, D. G. & Mysak, L. A. A zonally averaged, coupled ocean–atmosphere model for paleoclimate studies. *J. Clim.* **5,** 773–797 (1992).
13. Rahmstorf, S. Bifurcations of the Atlantic thermohaline circulation in response to changes in the hydrological cycle. *Nature* **378,** 145–149 (1995).
14. Gleckler, P. J. *et al.* Cloud-radiative effects on implied oceanic energy transports as simulated by atmospheric general circulation models. *Geophys. Res. Lett.* **22,** 791–794 (1995).
15. Peltier, W. R. Ice age paleotopography. *Science* **265,** 195–201 (1994).
16. Schmitz, W. J. On the interbasin scale thermohaline circulation. *Rev. Geophys.* **33,** 151–173 (1995).
17. Macdonald, A. & Wunsch, C. An estimate of global ocean circulation and heat fluxes. *Nature* **382,** 436–439 (1996).
18. Toggweiler, J. R. & Samuels, B. in *The Global Carbon Cycle* (ed. Heimann, M.) 333–366 (Springer, Berlin, 1993).
19. Döös, K. The Deacon cell and the other meridional cells of the Southern Ocean. *J. Phys. Oceanogr.* **24,** 429–442 (1994).
20. Rahmstorf, S. On the freshwater forcing and transport of the Atlantic thermohaline circulation. *Clin. Dyn.* **12,** 799–811 (1996).
21. Levitus, S., Burgett, R. & Boyer, T. *World Ocean Atlas 1994* Vol. 3, *Salinity* 1–150 (US Govt Printing Office, Washington DC, 1994).
22. Hall, M. M. & Bryden, H. L. Direct estimates and mechanisms of ocean heat transport. *Deep-Sea Res.* **29,** 339–359 (1982).
23. Stommel, H. Asymmetry of interoceanic freshwater and heat fluxes. *Proc. Natl Acad. Sci. USA* **77,** 2377–2381 (1980).
24. Manage, S. & Stouffer, R. J. Two stable equilibria of a coupled ocean–atmosphere model. *J. Clim.* **1,** 841–866 (1988).
25. Houghton, J. T. *et al.* (eds) *Climate Change 1995—The Science of Climate Change* (Cambridge Univ. Press, 1996).
26. Street-Perrot, F. A. & Harrison, S. P. in *Paleoclimate Analysis and Modeling* (ed. Hecht, A. D.) 291–340 (Wiley, New York, 1985).
27. Herron, M. M. & Langway, C. C. in *Greenland Ice Core: Geophysics, Geochemistry, and the Environment* (eds Langway, C. C., Oeschger, H. & Dansgaard, W.) 77–84 (Am. Geophys. Union, Washington DC, 1985).
28. Winkler, M. G. & Wang, P. K. in *Global Climates since the Last Glacial Maximum* (ed. Wright, H. E.) 221–264 (Univ. Minnesota Press, Minneapolis, 1993).
29. Hooghiemstra, H., Bechler, A. & Beug, H.-J. Isopollen maps for 18,000 years B.P. of the Atlantic offshore of Northwest Africa: Evidence for paleowind circulation. *Paleoceanography* **2,** 561–582 (1987).
30. Sarnthein, M. *et al.* Changes in east Atlantic deepwater circulation over the last 30,000 years: Eight time slice reconstructions. *Paleoceanography* **9,** 209–267 (1994).
31. Yu, E.-F., Francois, R. & Bacon, M. P. Similar rates of modern and last-glacial ocean thermohaline circulation inferred from radiochemical data. *Nature* **379,** 689–694 (1996).
32. Lynch-Stieglitz, J. & Fairbanks, R. G. A conservative tracer for glacial ocean circulation from carbon isotope and palaeonutrient measurements in benthic foraminifera. *Nature* **369,** 308–310 (1994).
33. Rahmstorf, S. Rapid climate transitions in a coupled ocean–atmosphere model. *Nature* **372,** 82–85 (1994).
34. Beckmann, A. & Döscher, R. A method for improved representation of dense water spreading over topography in geopotential-coordinate models. *J. Phys. Oceanogr.* **27,** 581–591 (1997).
35. Cubasch, U. *et al.* A climate change simulation starting from 1935. *Clim. Dyn.* **11,** 71–84 (1995).
36. Manabe, S. & Stouffer, R. J. Multiple-century response of a coupled ocean–atmosphere model to an increase of atmospheric carbon dioxide. *J. Clim.* **7,** 5–23 (1994).
37. Rahmstorf, S. Risk of sea-change in the Atlantic. *Nature* **388,** 825–826 (1997).
38. Stute, M. *et al.* Cooling of tropical Brazil (5 °C) during the last glacial maximum. *Science* **269,** 379–383 (1995).
39. Thompson, L. G. *et al.* Late glacial stage and holocene tropical ice core records from Huascaran, Peru. *Science* **269,** 46–50 (1995).
40. Beck, J. W., Récy, J., Taylor, F., Edwards, R. L. & Cabioch, G. Abrupt changes in early holocene tropical sea surface temperature derived from coral records. *Nature* **385,** 705–707 (1997).
41. Guilderson, T. P., Fairbanks, R. G. & Rubenstone, J. L. Tropical temperature variations since 20,000 years ago: Modulating interhemispheric climate change. *Science* **263,** 663–665 (1994).
42. Broecker, W. S. Oxygen isotope constraints on surface ocean temperatures. *Quat. Res.* **26,** 121–134 (1986).
43. Peyron, O. *et al.* Climatic reconstruction in Europe from pollen data, 18,000 years before present. *Quat. Res.* (in the press).
44. Guiot, J., Pons, A., de Beaulieu, J. L. & Reille, M. A 140,000 year climatic reconstruction from two European records. *Nature* **338,** 309–313 (1989).
45. Jäger, L. *Monatskarten des Niederschlags für die ganze Erde, Ber. Deutschen Wetterdienstes* No. 139, 1–38 (1976).
46. Hellerman, S. & Rosenstein, M. Normal monthly wind stress over the world ocean with error estimates. *J. Phys. Oceanogr.* **13,** 1093–1104 (1983).

Acknowledgements. S.R. and M.C. acknowledge discussions with S. Joussaume, A. Broccoli and others at the European Science Foundation's Research Conference on Paleoclimate Modelling and Analysis, in Castelvecchio Pascoli. We received comments on the manuscript from E. Bard; D. Smart critically read the manuscript. This work was supported by the European Union's Environment and Climate programme.

Correspondence and requests for materials should be addressed to S.R. (e-mail: rahmstorf@pik-potsdam.de).